ANTICANCER RESEARCH *24*: 187-198 (2004)

Computational Simulation of Chronic Persistent Virus Infection: Factors Determining Differences in Clinical Outcome of HHV-6, HIV-1 and HTLV-1 Infections Including Aplastic, Hyperplastic and Neoplastic Responses

G.R.F. KRUEGER[1], M.E. BRANDT[2], G. WANG[3] and L.M. BUJA[3]

[1]Department of Internal Medicine and
[3]Department of Pathology and Laboratory Medicine,
University of Texas-Houston Medical School, Houston, Texas 77030;
[2]Center for Computational Biomedicine, University of Texas-Health Science Center at Houston,
Houston, Texas 77030, U.S.A.

Abstract. *A computational model was recently designed to simulate cellular changes in the T cell immune system. The model was validated by simulating cell changes in viral infections which target the same CD4+ T cell, yet cause either hyperplastic, aplastic or neoplastic responses. Respective case material for comparison was available from human infections with human herpesvirus-6 (HHV-6), human immunodeficiency virus (HIV-1) or human T cell leukemia virus (HTLV-1). Starting with cell values for a healthy human individual, factorial changes that influence the individual course of the various infections were determined by an algorithm search procedure. Such factorial differences determining a clinical course with aplasia, hyperplasia or neoplasia are outlined and further discussed in this paper.*

We have recently designed and validated a computational model for simulating T cell dynamical changes in order to study cell proliferation, differentiation and cell death in infectious and neoplastic diseases (1-3). The model is based upon cells shifting from immature to mature cell pools under the influence of various factors and feedback-feedforward mechanisms according to current concepts of the T cell immune system and using standard textbook data (4-9). The value and clinical implications of feedback-feedforward mechanisms were discussed in detail in a separate publication (10). The proposed model has also proven useful for simulating cellular changes in acute and chronic viral infections as well as in cases of pseudolymphomatous lymphoproliferation, *i.e.* the Canale-Smith syndrome (2,3,11). The present report investigates factorial differences in the model and their possible biological implications with respect to hyperplastic, aplastic and neoplastic responses. Prototype viral infections introduced into this study are infections with HHV-6, HIV-1 and HTLV-1 (12-15), all of which target the CD4+ T cells yet cause different disease patterns.

Correspondence to: Gerhard R.F.Krueger, MD, PhD, Department of Internal Medicine, University of Texas-Houston Medical School, 6431 Fannin St., MSB 2.246, Houston Texas 77030 U.S.A. Tel: 713-500 7874, Fax: 713-500 0730, e-mail: Gerhard.Krueger@uth.tmc.edu

Key Words: Computational simulation, infection, HHV-6, HIV, HTLV-1, clinical course.

Materials and Methods

Basic simulation model. The basic conceptional model as previously validated and published (1-3) is presented in Figures 1 and 2 with its mathematical representation in equation [1]. Detailed stability

$$\begin{aligned} w &= \mu_w + w\left(\sum_{h=1}^{H} P_{wh} - \sum_{j=1}^{J} D_{wj} - \sum_{k=1}^{K} I_{wk} + ax - by + cz\right) \\ x &= \mu_x + x\left(\sum_{l=1}^{L} P_{xl} - \sum_{m=1}^{M} D_{xm} - \sum_{n=1}^{N} I_{xn} - dy + ez\right) + fw \\ y &= \mu_y + y\left(\sum_{q=1}^{Q} P_{yq} - \sum_{r=1}^{R} D_{yr} - \sum_{s=1}^{S} I_{ys} + gz\right) + ux \\ z &= \mu_z + z\left(\sum_{\theta=1}^{\Theta} P_{z\theta} - \sum_{\omega=1}^{\Omega} D_{z\omega} - \sum_{\gamma=1}^{\Gamma} I_{z\gamma}\right) + \delta y \end{aligned} \qquad [1]$$

testing confirmed the practicality of the modeling approach (3). The model functions in a circular ring-type network configuration with feedforward and feedback connections expressed as a system of four interrelated ordinary differential equations (ODEs). Notations used are as follows (see also Tables I and II):

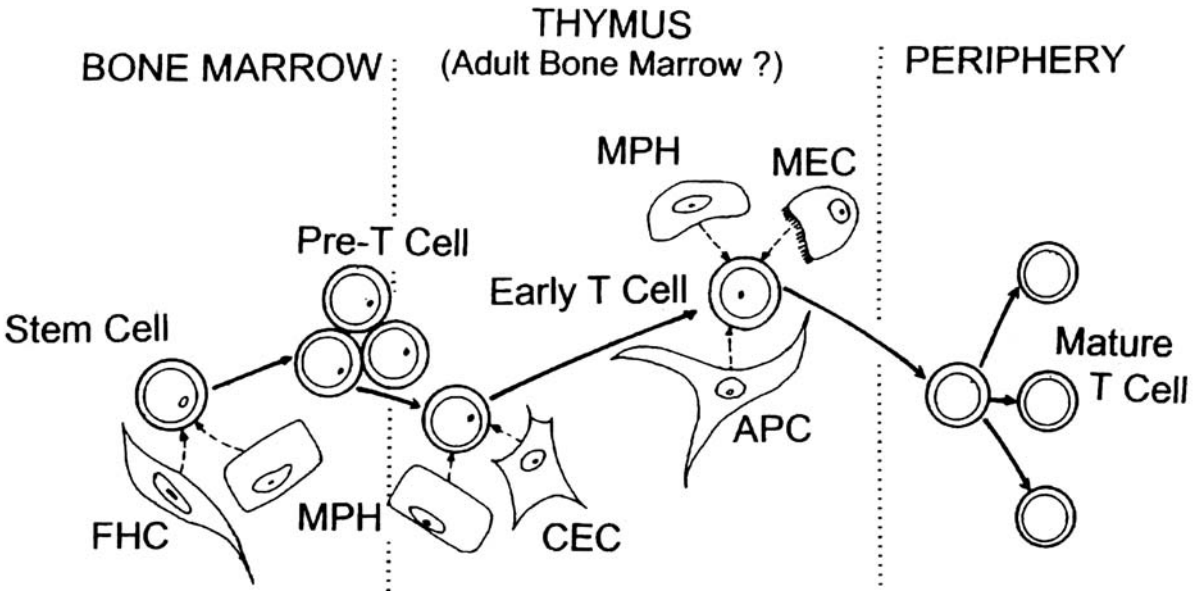

Figure 1. *Basic steps in T cell maturation and microenvironmental influences: stem cells from the bone marrow enter and move through the thymus, where they expand and undergo maturation and selection under the influence of factors from epithelial cells, macrophages and antigen-presenting cells. They leave the thymus into the periphery (blood and lymphoid tissues) as mature virgin lymphocytes. (FHC: fibrohistiocyte; MPH: macrophage; CEC: cortical epithelial cell; MEC: medullary epithelial cell; APC: antigen-presenting cell)*

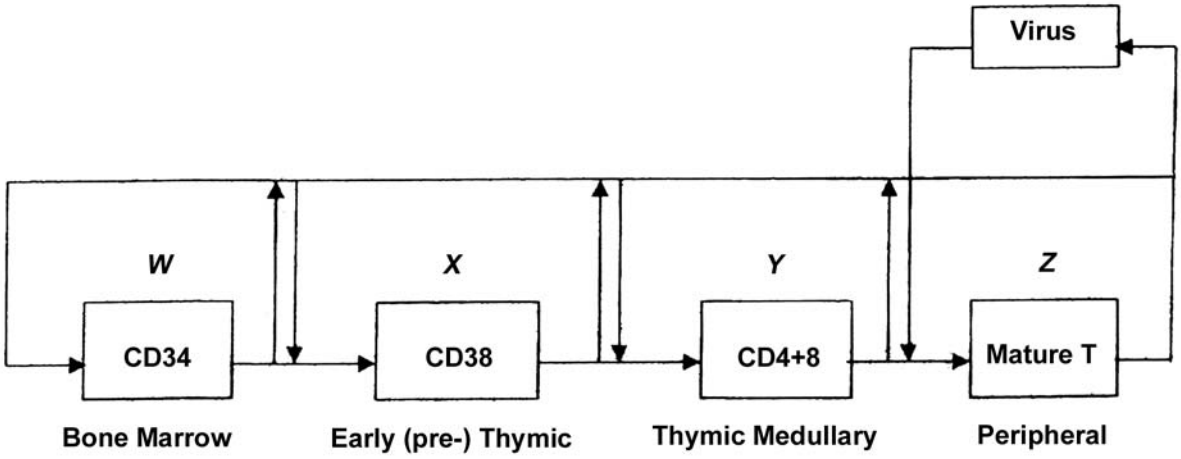

Figure 2. *Simplified bloc diagram of computer model for virus infection.*

w, x ,y, z T cell pools (stem cell, immature & mature) in bone marrow, thymic cortex, thymic medulla and periphery; the dot notation indicates a time rate of change of cell numbers in each pool (*e.g. dw/dt*).

P, D, I a set of factors regulating proliferation, differentiation and inhibition in pools *w, x, y* and *z*. Each separate factor is represented by a real number and they are lumped summation as implemented and shown in equation [1]. .

μ [w-z] average regeneratory potential of each compartment.

a-g,u,δ are scalar gains (strength) of the feedforward and feedback connections within and between cell pools. Their implications have been discussed in detail in another publication (10).

The model's feedback terms are implemented as a multiplication of the state variable of the compartment itself, the inflow from the forward compartment and a compartmental cross-renewal rate implemented as a scalar gain term. In this sense, *a-g, u* and *δ* represent virtual values for the "strength of connections" between

Table I. *Base model parameters for simulating normal T cell pools across the life-span.*

Factor	Value	Definition
$w(t_0)$	100.0	stem cell pool in the bone marrow
$x(t_0)$	1.0 x 10^4	cortical (early) thymus lymphocyte cell pool
$y(t_0)$	1.0 x 10^7	medullary (late) thymus lymphocyte pool
$z(t_0)$	1.0 x 10^5	peripheral mature T cell pool (all)
μ_w	50.0	regeneratory potential of bone marrow stem cells
μ_x	25.0	regeneratory potential of cortical thymic lymphocytes
μ_y	2.5 x 10^6	regeneratory potential of medullary thymic lymphocytes
μ_z	1.0 x 10^4	regeneratory potential of peripheral mature lymphocytes
P_w - D_w - I_w	-0.531	self-feedback (memory) of bone marrow pool
P_x - D_x - I_x	-0.04	self-feedback (memory) of thymic cortical cell pool
P_y - Dy - Iy	-0.7	self-feedback (memory) of thymic medullary cell pool
P_z - D_z - I_z	-0.023	self-feedback (memory) of peripheral T cell pool
a	5.0 x 10^{-7}	feedback thymic cortex to bone marrow
b	2.0 x 10^{-7}	feedback thymic medulla to bone marrow
c	5.0 x 10^{-7}	feedback periphery to bone marrow
d	-5.5 x 10^{-8}	feedback thymic medulla to thymic cortex
e	3.6 x 10^{-7}	feedback periphery to thymic cortex
f	5.0 x 10^{-7}	eedforward bone marrow to thymic cortex
g	1.0 x 10^{-7}	feedback periphery to thymic medulla
u	0.05	feedforward thymic cortex to thymic medulla
δ	0.001	feedforward thymic medulla to periphery

(Pool values were downsized exponentially while keeping the inter-pool relationships in order to keep computational working times within realistic limits; for the same reason, initial pool values at t_0 were adjusted from the text book values of $w = 10^5$; $x = 2.0 \times 10^7$; $y = 4.5 \times 10^{11}$ and $z = 8.0 \times 10^9$. All other values were determined by parameter search algorithm with the objective of retaining actual human cell pool data [see text])

pools, thus of feedback and feedforward mechanisms (see also Table I). Actual values under normal conditions (*i.e.* in the healthy individual) are found by use of both manual and semi-automated search procedures (parameter search algorithm; see appendix) during the model validation. The procedures were described in detail in a previous publication (3).

The model operates with textbook data for normal pool sizes (5-9). Simulations were carried out using Matlab software developed by us. The ODEs were solved using fourth-order Runge-Kutta integration. Each computer run was simulated continuously over a given timeframe, *e.g.*, for establishing the life-time values from birth (t_0=0) to the age of 80 years. Respective parameters for simulating a clinically normal human adult are given in Table I.

When substituting parameters from Table I into equations [1], one obtains the following set of ordinary differential equations [2]:

$$\begin{aligned}
\dot{w} &= 50.0 - 0.531w + (5.0 \times 10^{-7})wx - (2.0 \times 10^{-7})wy + (5.0 \times 10^{-7})wz,\\
\dot{x} &= 25.0 - 0.04x - (5.5 \times 10^{-8})xy + (3.6 \times 10^{-7})xz + (5.0 \times 10^{-7})w,\\
\dot{y} &= (2.5 \times 10^{6}) - 0.7y + 0.05x + (1.0 \times 10^{-7})yz,\\
\dot{z} &= (1.0 \times 10^{4}) - 0.023z + 0.001y.
\end{aligned} \qquad [2]$$

Model for simulating viral challenge. As it proved difficult to accommodate viral stimulation data within the basic model, we tried the standard sigmoid function for weighting since its smooth shape can be easily controlled by changing its two basic parameters (the slope of the sigmoid function) and (the time delay of the sigmoid function). This allows us to account for processes that may occur earlier or later than others. The modified model reads as follows:

$$\begin{aligned}
\mathbf{Z} &= \mu_z + z(P_z - D_z - I_z + k_2\psi_2 v) + \delta y + k_1\psi_1 v,\\
\mathbf{V} &= v(l_1\varrho_1 + l_2\varrho_2 z),
\end{aligned} \qquad [3]$$

In this model $\delta = 0.0$ to disengage the (v,z) subsystem from the basic system in order to simplify analysis. Sigmoidal relations are

$$\begin{aligned}
\psi_{1,2}(t) &= \frac{1}{1+\exp\left(\lambda_{1,2}(t-\tau_{1,2})\right)},\\
\rho_{1,2}(t) &= \frac{1}{1+\exp\left(\lambda'_{1,2}(t-\tau'_{1,2})\right)}.
\end{aligned} \qquad [4]$$

and the revised system with virus compartment added is:

$$\begin{aligned}
w &= \mu_w + w\left(P_w - D_w - I_w + ax + by + cz\right),\\
x &= \mu_x + x\left(P_x - D_x - I_x + dy + ez\right) + fw,\\
y &= \mu_y + y\left(P_y - D_y - I_y + gz\right) + ux,\\
z &= \mu_z + z\left(P_z - D_z - I_z + k_2\psi_2 v\right) + \delta y + k_1\psi_1 v,\\
v &= v(l_1\rho_1 + l_2\rho_2 z).
\end{aligned} \qquad [5]$$

If in this equation ψ_1 weights larger before time τ_1 than after time τ_1 , then viral antigenic stimulation is greater prior to τ_1 than afterward (for additional comments including parameter variation and tolerance of the system see ref. 3).

Simulated values used under conditions of viral infection were determined by use of both manual and semi-automated search procedures (parameter search algorithm; see appendix) during the

Table II. *Model parameters for simulating chronic persistent virus infections*.*

Factor	Values			Definition
	HHV-6	HIV-1	HTLV-1	
P_z - D_z - I_z *(CD4)*	-0.478	-0.223	nd	self-feedback (memory) of CD4 T cells
P_z - D_z - I_z *(CD8)*	-0.463	-0.511	nd	self-feedback (memory) of CD8 T cells
k	1.07×10^{-3}	7.13×10^{-8}		viral stimulus for CD8 T cell proliferation
k1	nd	nd	681.45	viral stimulus for mature T cell proliferation
k2	nd	nd	-0.0069528	T cell apoptosis upon viral infection
l	-5.6×10^{-4}	-8.84×10^{-4}	nd	CD8 cell apoptosis upon viral infection
l1	nd	nd	0.8786	virus replication by infected cells
l_2	nd	nd	-2.47x10-8	apoptosis of infected cells (& reduction of viral replication)
λ_1	0.0592/w	1.08/w	-0.21009/y	rate parameter of viral stimulation
λ_2	0.0352/w	0.04/w	0.16195/y	rate parameter of cell apoptosis by virus
λ'1	nd	0.2/w	-0.4054/y	rate parameter of virus production by CD4 cells
λ'2	nd	0.6/w	0.32535/y	rate parameter of CD8 cell killing of virus-infected CD4 cells
τ1	-0.0178w	-0.0106w	-7.682y	time parameter of virus stimulation
τ2	0.0122w	0.004w	-13.369y	time parameter of T cell apoptosis by virus
τ3	-0.015w	-0.0078w	nd	time parameter of CD8 cell death secondary to their cytotoxic activity
τ4	0.037w	-0.094w	nd	time parameter of CD8 cell stimulation by virus
τ'1	-0.0075w	-0.0142w	10.234y	time parameter of virus production by CD4 cells
τ'2	-0.001w	-0.000947w	9.888y	time parameter of CD8 cell killing of infected CD4 cells
τ'3	-0.00944w	-0.0092w	nd	time parameter of viral clearance
v(tvs)	3.8	3.8	0.1	viral challenge
μ (CD4)	321000	546000	nd	regeneratory potential of CD4 cells
μ (CD8)	127000	492000	nd	regeneratory potential of CD8 cells
i	-3.09×10^{-3}	-2.35×10^{-5}	nd	CD4 cell apoptosis following viral stimulus
j	0.01	9.0×10^{-4}	nd	CD4 cell proliferation upon viral contact
m	7.0×10^{-5}	6.7×10^{-5}	nd	virus production by CD4 cells
o	-3.14×10^{-7}	-1.47×10^{-7}	nd	inherent virus load reduction (not caused by cytotoxic CD8 cells)

* basic factors identified in Table I also apply to simulations of viral infections; this table shows additional factors to be considered.
nd: not done since no human data were available for comparison; y: year; w: week

model validation and in comparison to cell pool data in human patients with respective infections (3,16). All are thus virtual values found by systematically simulating conditions which ultimately lead to cell pool changes as observed in existing patients (13-15). They are summarized in Table II.

Results

Normal cell numbers in immature and peripheral T cell pools as obtained from equations 1 and 2 and the data in Table I are shown in Figure 3. As can be seen, there is a characteristic age-related decrease in peripheral T lymphocytes accompanied by respective changes in the thymic cortical lymphocyte pool. While thymic cortical lymphocytes increase during the first two decades of life and then gradually decrease, bone marrow stem cells and thymic medullary cells remain for the most part constant after initial adjustment after birth. Cell changes following simulated viral infections are depicted in Figure 4 and are shown in a connected (*i.e.* superimposed) way. They are discussed in more detail in previous publications (2,3). As Figure 4 shows, consistent with patients' data, chronic HHV-6 infection causes changes in peripheral T lymphocytes varying between hyperplasia and hypoplasia (13), while HIV-1 infection leads to severe peripheral lymphopenia (most pronounced in CD4 cells (14); and HTLV-1 infection causes late atypical T cell lymphocytosis indicative of adult T cell leukemia (15). Respective cell changes in the more immature pools are depicted in Figure 5. Stem cell numbers in the bone marrow *(w)* remain fairly constant after some initial postinfectious depression. To the contrary, cell numbers in the thymic cortex *(x)* steadily rise in all three viral infections, which was also reflected in the rising CD38 cell numbers in human patients (13-15). Cell numbers in the thymic medulla *(y),* however, decrease significantly suggesting some intrathymic maturation blockage.

Simulation of these model infections thus is well suited for comparative evaluation of characteristic factorial changes as summarized in Table II and may permit some additional clues as to functional disturbances in these viral infections.

When factorial changes in persistent HHV-6 infection as given in Table II are compared to those in HIV-1 infection, certain major differences between the two viral infections become evident:

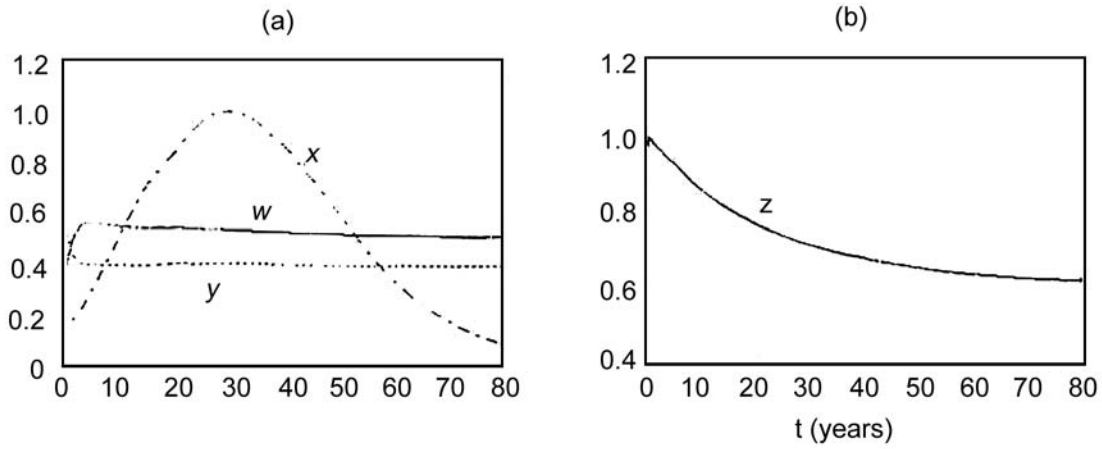

Figure 3. *Computer simulation run over a life-span of 80 years showing relative cell counts versus time for cell pools bone marrow (w), thymic cortex (x), thymic medulla (y) and peripheral T lymphocytes (z). Absolute cell counts were arbitrarily scaled to fit the graphs. The main feature was the slow exponential decrease of peripheral blood T lymphocytes across the life-span and changes in less mature cell pools corresponding to what occurs in normal healthy individuals (5).*

Comparison of persistent HHV-6 with HIV-1. As Table II and equations [3]-[5] show, having the same magnitude of initial viral challenge (*v[tvs]*) in HHV-6 and HIV infection, the viral stimulus for CD4 and CD8 cell proliferation (model parameters *j* and *k*) is significantly lower in HIV infection than in HHV-6 infection. Also, the rate parameter of viral stimulation per week (*i.e.* the intensity of stimulation; [λ1]) appears to be larger in HIV than in HHV-6 infection, and consequently changes in ψ indicate that viral stimulation subsides faster in HIV-1 than in HHV-6 infection . The time delay parameter (τ1 *i.e.* the time at which the strength λ has decreased or increased by 50%) is larger for HHV-6 than for HIV-1, signalling a slightly delayed response for HHV-6 as compared to HIV infection. The regeneratory potential appears higher for peripheral CD4 and CD8 cells in HIV-infected individuals. The production of new virus (virus replication by infected CD4 cells; [*m*] does not significantly differ in HIV and HHV-6 infection. The time-delay parameter of virus production by CD4 cells (τ'1), however, is larger in HHV-6 infection and smaller in HIV infection, which may account for the observed differences in T cell stimulation in both infections.

While the rate parameter per week of T cell killing by the virus (λ2) does not differ very much in the two infections, the time-delay parameter of T cell killing (τ2) is markedly larger in HHV-6 infection than in HIV, *i.e.* virus-induced T cell killing depending upon the respective λ value – subsides probably more rapidly in HHV-6 infection than in HIV-1 infection.

There appears to exist no significant difference in the time-delay parameter of the killing of virus-infected CD4 cells by cytotoxic CD8 lymphocytes in both diseases (τ'2), and cytotoxic CD8 cells tend to die somewhat more readily in HHV-6 infection than in HIV-1 *(1)*. This may suggest a somewhat more vigorous cytotoxic T cell response in HHV-6.

Considering any potential non-CD8 cell induced reduction of the viral load (*e.g.* by antibody or non-specific reactions), *i.e.* the "inherent virus load reduction [*o*] in HHV-6 is cleared about two times as readily as in HIV-1.

Finally, it is interesting to note, that there is apparently some reduced feedback memory in the peripheral CD4 cell pool (inherent memory of pool size; *[P_z-D_z-I_z CD4]*) in HIV as compared to HHV-6 infection and as compared to CD8 cell feedback in both infections.

Comparison of HTLV-1 infection with persistent HHV-6 and/or HIV-1. As opposed to HHV-6 and HIV-1, factorial parameters in HTLV-1 infection change slowly and over longer periods of time, *i.e.* in terms of years rather than weeks (see Table II). The rate parameter of viral stimulation (λ1) in HTLV-1 infection is increased as compared to HHV-6 and HIV-1. Similarly, the rate parameter for viral replication (λ'1) is larger for HTLV-1, yet smaller for HHV-6 and HIV-1 with a respective increase or decrease in the sigmoid functions ψ and ϱ. This may indicate a steadily increasing viral stimulation in HTLV-1 contrary to HHV-6 or HIV-1, however, the time-delay parameter for viral stimulation (τ1) in HTLV-1 infection also is large. The time parameter of viral replication (τ'1) for HTLV-1 is small, similar to HIV-1 but different to HHV-6, *i.e.* viral replication may steadily increase. It compares well to the exponential growth in certain T cell pools (Figures 4 and 5) and is much more pronounced for HTLV-1 than for HIV-1.

Both, the rate parameter and the time-delay parameter for the killing of HTLV-1-infected cells by cytotoxic CD8 T lymphocytes (τ'2 and λ'2) are remarkably small. In HIV-1 infection, instead, the time-delay parameter for CD8 T cell-mediated killing is increased, while the rate parameter is still small, *i.e.* the timing for effective killing of HIV-1-infected cells takes increasingly longer. Death of infected

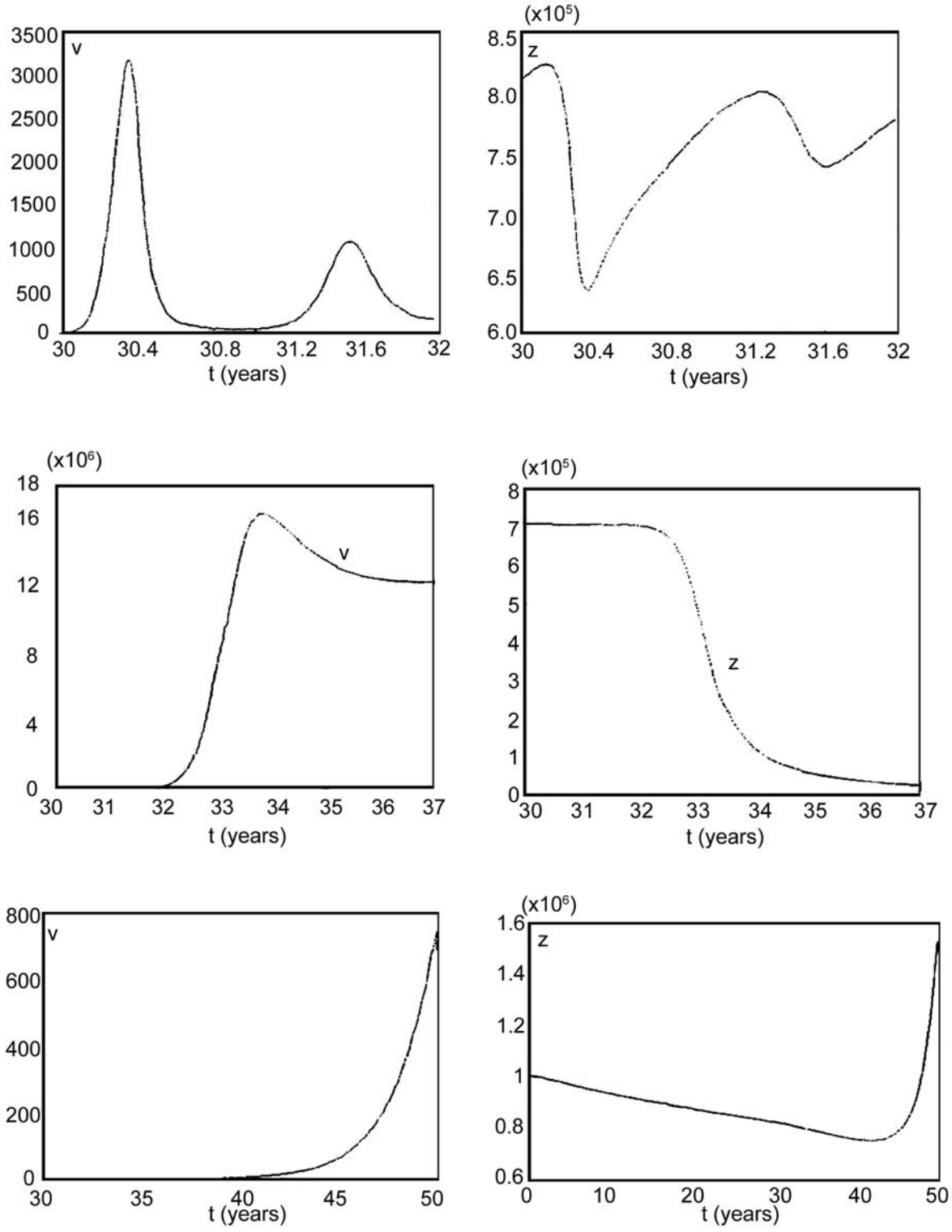

Figure 4. *Computer simulation runs for chronic persistent viral infection with HHV-6 (top), HIV-1 (center) and HTLV-1 (bottom) showing relative counts of peripheral T lymphocytes as related to viral DNA (HHV-6) or RNA (HIV, HTLV) mass (v) over time. HHV-6 infection occurred at age 30 years and was followed for 2 years. HIV-1 infection initiated at age 32 years and was followed for 5 years. HTLV-1 infection presumably also started at age of 30 years and was followed for 20 years. All peripheral T cell values (z) are shown in connected form to normative data, for HTLV-1 to include the normal cell data for the age groups before infection (i.e. 0-30 years). They correspond well to actual data as determined in human patients with respective viral infections (13-15).*

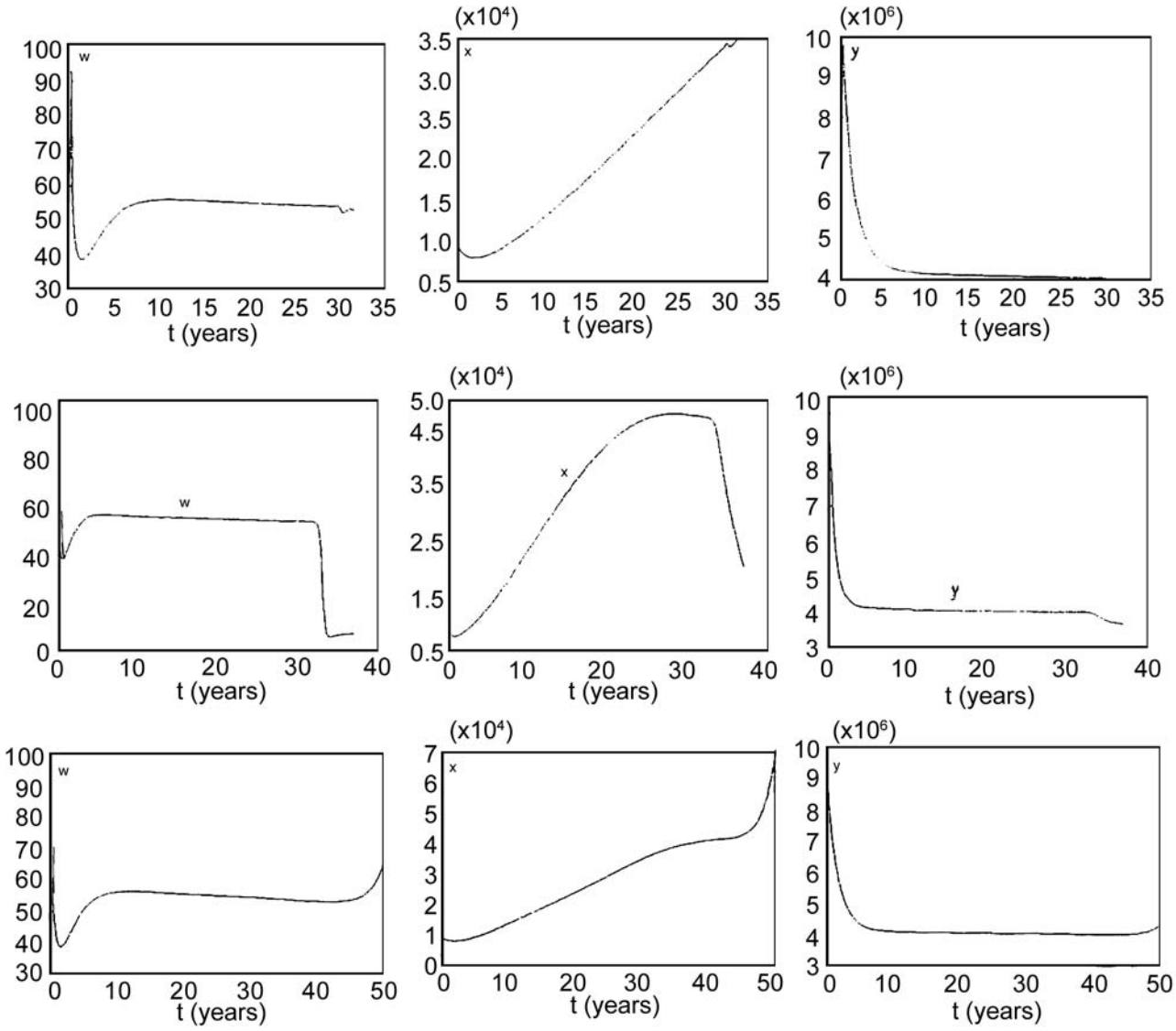

Figure 5. *Computer simulation runs for chronic persistent viral infection with HHV-6 (top), HIV-1 (center) and HTLV-1 (bottom) showing relative counts of cell pools in bone marrow (w), thymic cortex (x) and thymic medulla (y). This figure supplements Figure 4 showing the viral load and peripheral T cells.*

cells as immediate effect of the virus (*i.e.* virus-induced apoptosis; [$\lambda 2$ and $\tau 2$]) in HTLV-1 infection is overall decreased and takes progressively longer as their rate and time-delay parameters show. These changes are similar to HHV-6 and HIV rate parameters, although more pronounced in HTLV-1, yet they are reversed with respect to the time-delay parameters of HIV and HHV-6. The initial viral challenge in HTLV-1 is about 38 times lower than in the other two persistent viral infections.

Discussion

Human herpesvirus 6 (HHV-6), human immunodeficiency virus 1 (HIV-1) and human T cell leukemia virus 1 (HTLV-1) all infect similar cell populations, preferentially CD4 T helper cells (17-19), yet their clinical course is not similar: while HHV-6 usually causes acute infectious mononucleosis-like features or chronic persistent infections with chronic fatigue syndrome or autoimmune disorders (20), HIV-1

leads to the loss of CD4 T cells and to acquired immunodeficiency, AIDS (21). HTLV-1, instead, may cause a chronic persistent infection with topical spastic paraparesis or adult T cell leukemia (22). Although structurally different (HHV-6: DNA virus, HIV and HTLV-1: RNA viruses), their mode of replication does not readily explain the differences in their clinical courses. A significant contributory factor to such clinical differences may well be the distinct interplay with the immune system of these viruses. It appears, thus, intriguing to further investigate this assumption by means of computational modeling.

We have presented such a computational model previously for simulating cell pool data in the human T cell system under various conditions of infection, immunodeficiency and atypical cell proliferation (1-3). This model appeared well suited for a search for factorial influences upon T cell pools in virus infection, and for relating differences in such factors to differences in the clinical courses of individual infections.

After establishing and validating our computational model for T cell pool data in a healthy human individual over a life-time of 80 years, simulation runs were performed for acute HHV-6 infection and for persistent active infections with HHV-6, HIV-1 and HTLV-1.

Acute HHV-6 infection (2,3) is characterized by a transient severe hyperplastic response of T lymphocytes corresponding to blood lymphocytosis in infectious mononucleosis (23). The stimulus of the immune system by HHV-6 is short-lived and intense with up to 8.2 x log10 viral DNA copies per 5 μL blood for about 8-12 weeks (12). The rate parameter (strength) of viral stimulation of the immune system (not shown in the Table) is very high (35.6602/y), as is the transient rate parameter of HHV-6 production by CD4 cells (35.8895/y). However, similarly intense is the rate parameter (strength) of CD8 killing of HHV-6-infected CD4 cells (-41.3943/y) indicating a very vigorous cellular immune response which leads to a rapid reduction of infectious virus. Simulation data as published before (2,3) are explanatory for the acute clinical course and recovery of the patients.

Chronic persistent HHV-6 infection as compared to acute HHV-6 follows a rather protracted course with a variable T cell response (hyperplastic, hypoplastic or normal) such as described in certain cases of postinfectious chronic fatigue syndrome (13,24). Virus clearance from the peripheral blood remains incomplete over longer periods of time with variable numbers of DNA copies (1.0-6.4 x log10/5μL blood). Such persistent activity of virus is thought to be caused by a so far ill-defined immune deficiency (24-30). Our simulation data concur with the *in vivo* findings, namely that viral challenge and stimulation of the immune system in acute HHV-6 infection are much larger than in chronic HHV-6, yet of short duration in acute infection as opposed to the long lasting low level stimulation in chronic HHV-6. Intense viral exposure of short duration thus apparently causes the markedly elevated lymphocyte proliferation in acute infection as known in infectious mononucleosis, while a more persistent viral exposure over longer periods of time will cause a rather moderate and variable lymphocytosis such as in chronic fatigue syndrome. The intensity of virus-induced apoptosis of T cells is larger in acute infection than in chronic HHV-6 with a respectively high rate of CD8 cell killing of infected CD4 cells and a low time-delay parameter for the killing of virus-infected cells. Thus virus replication is stopped much faster with respective virus clearing in acute HHV-6 infection than in chronic infection.

Human cases of ***HIV-1 infection*** as used for validation and for comparison with our simulation data were exclusively early cases without specific antiviral treatment and with a rapidly progressive course (14). These cases were thought to be representative for a natural course of the virus infection without any therapy effects. HIV-1 infections differ from chronic HHV-6 by their early and more pronounced impairment of immune defense followed by a "lethal" decline of CD4 T helper cells (Figures 4, 5; refs (21, 31-35)). The dynamics of HIV-1 virus load and respective CD4 cell changes have been successfully studied in previous mathematical model systems (36-41). Although they are able to simulate peripheral cell changes and their function in HIV infections, and were used in part to simulate possible therapeutic responses, they do not shed more light on the complexity of HIV-associated immune deficiency. In a computational model proposed by Nelson and Perelson (42), it is assumed that mechanisms of viral transfer to HIV-specific CD4 cells may allow slow-replicating HIV strains to escape an adequate immune response. Others attributed the developing immune deficiency more to a rapidly proliferating cell subpopulation undergoing apoptosis upon viral stimulation (43). When comparing our simulation data for chronic HHV-6 infection with those of HIV infection, there appear to be no major differences in the rate parameter of viral replication, viral production by CD4 cells and virus-induced cell killing (apoptosis). Viral stimulation of the immune system, however, seems about 20 times lower in HIV than in HHV-6 infection (Table II), and apoptosis appears to progress more rapidly in HIV-infected cells than in HHV-6 ones. Time-delay parameters for both viral stimulation and viral replication are small in HIV, yet large in chronic HHV-6 infection. The efficiency of CD8 cell-mediated killing of virus-infected cells is equal in both infections. In essence, HIV infections and its effects resemble more an acute infection of long duration than chronic persistent infection such as in persistent HHV-6. Different from acute HHV-6 – as an example of an acute infection of short duration – acute HIV of long duration

shows a significantly lower rate parameter of viral stimulation, *i.e.* the responsiveness of immunocompetent cells to HIV appears decreased permitting the virus a longer survival. Consequently, viral effects such as intensity and duration of viral stimulation will increase with time as shown by our simulation runs. Decreased responsiveness to HIV appears to be an early event before major CD4 T helper cell loss is notable, and its causes should probably be found on the level of cells interacting with the virus particle (receptor and/or membrane effect ?). Although our computer simulation data cannot further elucidate the complex intracellular behavior of HIV-1 (44), they may contribute certain aspects for studying the viral interference with immunocompetent cells and to the phenomenon that the degree of immune deficiency in HIV-infected persons does not necessarily correlate to the quantitative loss of CD4 T helper cells. One pathogenetic mechanism may consist of HIV stimulating preferentially the proliferation of naive T lymphocytes (45), which are infectable and support virus replication, yet cannot mount the efficient immune defense as memory T lymphocytes. In addition, the decreased cellular responsiveness to HIV as suggested by our studies may be related to alterations in the HIV-HLA interactions at the cellular level (46,47).

Data and case material of ***infections with HTLV-1*** were extracted from literature searches and are necessarily less homogeneous than the case material for HHV-6 and HIV-1 infections (15). This was necessary, however, since no data were available which could have been readily used for computational studies. Also, only data for HTLV-1-infected cases were used for validation and simulation studies, which terminated in the development of adult T cell leukemia, so that they could serve as an example for neoplastic cell pool changes in our simulation efforts. This represents about 2%-5% of all HTLV-1-infected persons (48-51). Our simulation data for HTLV-1 infection are strikingly different from those of HIV-1 and persistent HHV-6 infection and compare well to the clinical course of HTLV-1 with the development of adult T cell leukemia (15, 44-46).

Viral stimulation of the immune system occurs with high intensity, yet after extended periods of time which correspond to the viral replicative activities (Figure 4) with respective rate and time-delay parameters. This occurs, although the initial virus challenge is significantly lower for many years than all other infections we investigated in this study. However, the T cell death both by the virus and by cytotoxic CD8 cells is reduced as compared to HIV-1 and HHV-6, although the time-delay parameter for cell killing is small as in the other infections. This may signal that the induction of the killing process by the effector is unaltered, yet the response reduced. This observation is well in keeping with reports of an apoptosis blockade by HTLV-1 in transformed cells (52-55).

In summary, computer simulation studies, as described in this article, can be useful to gain additional understanding for regulatory disturbances in the immune system. In the present study this is shown for T cell pool data and various viral infections. In HTLV-1 infection as well as in others, such simulations may shed some light on functional disturbances preceding lymphoma development (11) or autoimmunity. They may also serve to plan more specific studies into the pathogenesis of T cell immune disorders or to design new regimens for therapeutic intervention.

Appendix: The Parameter Search Algorithm (16)

We describe our parameter search algorithm as applied to Eqs. [B], the *z - v* subsystem (virus and the peripheral compartment only). There are 12 parameters then that need to be searched/optimized. We use an optimization method that involves the minimization of an objective function defined as:

$$J(P) = \sum_{i}^{N} \left([z(P, ih) - z_i]^2 + [v(P, ih) - v_i]^2 \right), \qquad \text{(A1)}$$

where

$$P = (p_1, p_2, ..., p_{12}) = (k_1, k_2, l_1, l_2, \lambda_1, \lambda_2, \lambda_1', \lambda_2', \tau_1, \tau_2, \tau_1', \tau_2')$$

is the set of parameters to be determined, N is the total number of the samples, h is the numerical integration time interval between these samples, $z(P, t)$ and $v(P, t)$ are the concentrations of T cells and virus as functions of time, which are generated by Eqs. [2] under the parameter set p. z_i and v_i (for $i = 0, 1, ..., N$) are actual measured human data. The aim is to minimize the objective $J(P)$ by changing the twelve parameters respectively. That is, we first increase p_1 by a value Δp_1. If this action makes the objective function smaller, we continue doing this until the objective function changes sign. We then divide Δp_1 in half and repeat the abovementioned procedure. By doing this we reach a point that changing p_1 no longer affects the objective very much. We then in turn alter $p_2, p_3, ..., p_{12}$. In this way, the objective function is minimized at least to its local minima. The detailed procedure is summarized as follows:

Step 1. Set $j = 0$.

Step 2. Arbitrarily choose initial values for the parameters, $P = (p_1, ..., p_{12})$, with which Eqs. [3] are solved by the fourth order Runge-Kutta algorithm. $J(P)$ is obtained by Eq. (A_1) above.

Step 3. $j + 1 \rightarrow j$, if j reaches 13, stop.

Step 4. Increase p_j by a value m, *i.e.*, $P_m = (p_1, ..., p_j + m, ..., p_{12})$. Obtain $J(P_m)$ following the same procedure as Step 2.

Step 5. If $|J(P) - J(P_m)| < \varepsilon$ (a given small value), then $P_m \rightarrow P$, and then go to Step 3. Otherwise go to Step 6.

Step 6. If $J(P) - J(P_m) > 0$, then $P_m \rightarrow P$, and then go to Step 4. Otherwise make $-m/2 \rightarrow m$(change sign and halve the step size), then $Pm \rightarrow P$, and then go to Step 4.

Steps 1-6 guarantee the algorithm to converge to a local minimal. If the result is still unsatisfactory, we re-run the optimization algorithm using another set of values as initial parameters. By doing so we may jump out of the previous local minimal and obtain a better result. Since the dimension of the $z - v$ subsystem is 12, the optimization algorithm is very time consuming (running an a PIII PC). Furthermore, it is not easy to choose the correct initial values. Usually it converges to the original local minimal even after dozens of mutations.
[see also reference (16)]

References

1 Brandt ME, Wang G, Krueger GRF and Buja LM: A biodynamical regulatory model of the human T-cell system. Eng Med Biol (EMBS) Conf, Oct 20-23, 2002, Houston, Texas; Proc. 2nd Joint Conf IEEE EMBS-BMES, pp 254-255, 2002.

2 Krueger GRF, Brandt ME, Wang G and Buja LM: TCM-1: a nonlinear dynamical computational model to simulate cellular changes in the T cell system: conceptional design and validation. Anticancer Res *23*: 123-136, 2003.

3 Brandt ME, Krueger GRF, Wang G and Buja LM: A biodynamical model of human T-cell development and pathology: design, testing and validation. Chap20. *In*: Kaiser HE. Cancer Growth and Progression. 2nd ed, vol 4, Kluwer Acad Publ, Dordrecht, NL, 2004.

4 Benoist C and Mathis D: T-lymphocyte differentiation and biology. *In*: Paul WE: Fundamental Immunology. Lippincott-Raven, Philadelphia 367-409, 1999.

5 Krueger GRF: Klinische Immunpathologie. Stuttgart, W Kohlhammer, 1985.

6 Ogawa T, Kitagawa M and Hirokawa K: Age-related changes of human bone marrow: a histometric estimation of proliferative cells, apoptotic cells, T cells, B cells and macrophages. Mech Ageing Develop *117*: 57-68, 2000.

7 Wickenhauser C, Thiele J, Kuemmel T and Fischer R: Die haematopoietische Stammzelle des Menschen. Pathologe *16*: 1-10, 1995.

8 Erkeller-Yuksel FM, Deneys V, Yuksel B, Hannet I, Hulstaert F, Hamilton C, Mackinnon H, Turner Stokes L, Munhyeshull V, Vanlangendonck F, De Bruyere M, Bach BA and Lydyard PM: Age-related changes in human blood lymphocyte subpopulations. J Pediatr *120*: 216-222, 1992.

9 Hulstaert F, Hannet I, Denneys V, Munhyeshull V, Reichert T, De Bruyere M and Strauss K: Age-related changes in human blood lymphocyte subpopulations. II. Varying kinetics of percentage and absolute count measurements. Clin Immunol Immunopathol *70*: 152-158, 1994.

10 Brandt ME, Krueger GRF, Wang G and Buja LM: Investigating feedforward and feedback mechanisms among T cell pools using a biocomputational analysis. Submitted to J Clin Immunol, 2003.

11 Krueger GRF, Brandt ME, Wang G, Berthold F and Buja LM: A computational analysis of Canale-Smith syndrome: chronic lymphadenopathy simulating malignant lymphoma. Anticancer Res *22*: 2365-2372, 2002.

12 Krueger GRF, Bertram G, Ramon A, Koch B, Ablashi DV, Brandt ME, Wang G and Buja LM: Dynamics of infection with human herpesvirus-6 in EBV-negative infectious mononucleosis: data acquisition for computer modeling. In Vivo *15*: 373-380, 2001.

13 Krueger GRF, Koch B, Hoffmann A, Rojo J, Brindt ME, Wang G and Buja LM: Dynamics of chronic active herpesvirus-6 infection in patients with chronic fatigue syndrome: data acquisition for computer modeling. In Vivo *15*: 461-466, 2001.

14 Krueger GRF, Koch B, Denninger J, Tymister G, Ramon A, Brandt ME, Wang G and Buja LM: Dynamics of active progressive infection with HIV1: data acquisition for computer modeling. In Vivo *15*: 513-518, 2001.

15 Krueger GRF, Brandt ME, Wang G and Buja LM: Dynamics of HTLV-1 leukemogenesis: data acquisition for computer modeling. In Vivo *16*: 87-92, 2002.

16 Lewis RM, Torczon V, Trosset MW: Direct search method: then and now. J Comput Applied Math *124*: 191-207, 2000.

17 Lusso P: Target cells for infection. *In*: Ablashi DV, Krueger GRF, Salahuddin SZ (eds.): Human Hersepesvirus-6, Epidemiology, Molecular Biology and Clinical Pathology. Elsevier Sci Publ, Amsterdam 1992, pp. 25-36.

18 Klatzman D, Barre-Sinoussi F and Nugyere MT: Selective tropism of lymphadenopathy associated virus (LAV) for helper T-lymphocytes. Science *225*: 59-63, 1984.

19 Richardson JH, Edwards AJ, Cruikshank JK, Rudge P and Dalgleish AG: *In vivo* cellular tropism of human T-cell leukemia virus type 1. J Virol *64*: 5682-5687, 1990.

20 Salahuddin SZ, Kelley AS, Krueger GRF, Josephs SF, Gupta S and Ablashi DV: Human herpesvirus-6 (HHV-6) in diseases. Clin Diagn Virol *1*: 81-100, 1993.

21 Fauci AS and Clifton H: Human immunodeficiency virus (HIV): AIDS and related disorders. *In*: Harrison's Principles in Internal Medicine, 15th edition, McGraw Hill, Philadelphia, 2001, pp 1131-1135.

22 Blayney DW, Blattner WA, Jaffe ES and Gallo RC: Retrovirus in human leukemia. Hematol Oncol *1*: 193-204, 1983.

23 Steeper TA, Horwitz CA, Ablashi DV, Salahuddin SZ, Saxinger C, Saltzman R and Schwartz B: The spectrum of clinical and laboratory findings resulting from HHV-6 in patients with mononucleosis-like illnesses not resulting from EBV or CMV. Am J Clin Pathol *93*: 766-783, 1990.

24 Wagner M, Krueger GRF, Ablashi DV, Whitman JE and Rojo J: Chronic fatigue syndrome (CFS): Review of clinical data from 107 cases. Rev Med Hosp Gen, Mexico *61*: 195-210, 1998.

25 Gupta S and Vayuvegula B: A comprehensive immunologic analysis in chronic fatigue syndrome. Scand J Immunol *33*: 319-327, 1991.

26 Mawle AC, Nisenbaum R, Dobbins JG, Gary HE, Stewart JA, Reyes M, Steele L, Schmid DS and Reeves WC: Immune responses associated with chronic fatigue syndrome: a case-control study. J Infect Dis *175*: 136-141, 1997.

27 Whiteside TL and Friberg D: Natural killer cells and natural killer cell activity in chronic fatigue syndrome. Am J Med *105 (3A)*: 28S-34S, 1998.

28 Hanson JS, Gause W and Natelson B: Detection of immunologically significant factors for chronic fatigue syndrome using neural-network classifyers. Clin Diagn Lab Immunol *8*: 658-662, 2001.
29 Patarca-Montero R, Antoni M, Fletcher MA and Klimas NG: Cytokine and other immunologic markers in chronic fatigue syndrome and their relation to neuropsychological factors. Appl Neuropsychol *8*: 51-64, 2001.
30 Hilgers A and Frank J: Chronic fatigue syndrome: immune dysfunction, role of pathogens and toxic agents and neurological and cardial changes (in German). Wien Med Wschr *144*: 399-406, 1994.
31 Krueger GRF, Ablashi DV, Lusso P and Josephs SF: Immunological dysregulation of lymph nodes in AIDS patients. Curr Topics Path *84/2*: 157-188, 1991.
32 Galetto-Lacour A, Yerly S, Perneger PV, Baumberger C, Hirschel B and Perrin L: Prognostic value of viremia in patients with long-standing human immunodeficiency virus infection. Swiss HIV cohort study group. J Infect Dis *173*: 1388-1393, 1996.
33 Lathey JL, Hughes MD, Fiscus SA, Pi T, Jackson JB, Rasheed S, Elbeik T, Reichman R, Japour A, D'Aquila RT, Scott W, Griffith BP, Hammer SM and Katzenstein DA: Variability and prognostic values of virologic and CD4 cell measures in human immunodeficiency virus type 1-infected patients with 200-500 CD4 cells/mm(3) (ACTG 175). AIDS clinical trials group protocol 175 team. J Infect Dis *177*: 617-624, 1998.
34 Fahey JL, Taylor JM, Manna B, Nishanian P, Aziz N, Giorgi JV and Detels R: Prognostic significance of plasma markers of immune activation, HIV viral load and CD4 T-cell measurements. AIDS *12*: 1581-1590, 1998.
35 Rossi G, Donishi A, Casari S, Re A, Cadeo G and Carosi G: The international prognostic index can be used as a guide to treatment decisions regarding patients with human immunodeficiency virus-induced systemic non-Hodgkin lymphoma. Cancer *86*: 2391-2397, 1999.
36 Zorzenon dos Santos RM and Coutinho S: On the dynamics of the evolution of HIV infection. arXiv:cond-mat/0008081, Aug.4, 2000 (see also 37).
37 Zorzenon dos Santos RM and Coutinho S: Dynamics of the HIV infection: a cellular automata approach. Phys Rev Lett *89*: 219805, 2002.
38 Brandt ME and Chen G: Feedback control of a biodynamical model of HIV-1. IEEE Trans Biomed Engin *48*: 754-759, 2001.
39 Lederman MM, Kalish LA, Asmuth D, Fiebig E, Mileno M and Busch MP: Modeling relationships among HIV-1 replication, immune activation and CD4+ T-cell losses using adjusted correlative analyses. AIDS *14*: 951-958, 2000.
40 Kohler B, Puzone R, Seiden PE and Celada F: A systematic approach to vaccine complexity using an automaton model of the cellular and humoral immune system. I. Viral characteristics and polarized responses. Vaccine *19*: 862-876, 2001.
41 Kaufman GR, Zaunders J, Murray J, Kelleher AD, Lewin SR, Solomon A, Smith D and Cooper DA: Relative significance of different pathways of immune reconstritution in HIV type 1 infection as estimated by mathematical modeling. AIDS Res Hum Retrovir *17*: 147-159, 2001.
42 Nelson GW and Perelson AS: A mechanism of immune escape by slow-replicating HIV strains. J Acquir Immune Def Syndr *5*: 82-93, 1992.
43 Kovacs JA, Lempicki RA, Sidorov IA, Adelsberger JW, Herpin B, Metcalf JA, Sereti I, Polis MA, Davey RT, Travel J, Falloon J, Srevens R, Lambert L, Dewar R, Schwartzendruber DJ, Anver MR, Baseler MW, Masur H, Dimitrov DS and Lane HC: Identification of dynamically distinct subpopulations of T lymphocytes that are differentially affected by HIV. J Exp Med *194*: 1731-1741, 2001.
44 Chicurell M: Probing HIV's elusive activities within the host cell. Science *290*: 1876-1879, 2000.
45 Grossman Z and Paul WE: The impact of HIV on naive T-cell homeostasis. Nature Med *6*: 976-977, 2000.
46 Moore CB, John M, James IR, Christiansen FT, Witt CS and Mallal SA: Evidence of HIV-1 adaptation to HLA-restricted immune response at a population level. Science *296*: 1439-1443, 2002.
47 McMichael A and Klenerman P: HLA leaves its footprints on HIV. Science *296*: 1410-1411, 2002.
48 Ehrlich GD and Poiesz BJ: Clinical and molecular parameters of HTLV-I infection. Clin Lab Med *8*: 65-84, 1988.
49 Ikeda S, Momita S, Amagasaki T, Tsukasaki K, Yamada Y, Kusumoto Y, Ito M, Kanda N, Tomonaga M and Soda H: Detection of preleukemic state of adult T-cell leukemia (pre-ATL) in HTLV-1 carriers. Cancer Detect Prev *14*: 431-435, 1990.
50 Chen YX, Ikeda S, Mori H, Hata T, Tsukasaki K, Momita S, Yamada Y, Kamihira S, Mine M and Tomonaga M: Molecular detection of pre-ATL state among healthy HTLV-1 carriers in an endemic area of Japan. Int J Cancer *60*: 789-801, 1995.
51 Gabet AS, Mortreux F, Talarmin A, Plumelle Y, Lequercq I, Leroy A, Gessain A, Clity E, Joubert M and Wattel E: High circulating proviral load with oligoclonal expansion of HTLV-1 bearing T cells in HTLV-1 carriers with strongyloidiasis. Oncogene *19*: 4954-4960, 2000.
52 Tsuda H, Huang RW and Takatsuki K: Interleukin-2 prevents programmed cell death in adult T cell leukemia cells. Jpn J Cancer Res *84*: 431-437, 1993.
53 Copeland KF, Haaksma AG, Goudsmith J, Krammer PH and Heeney JL: Inhibition of apoptosis in T cells expressing human T cell leukemia virus type I tax. AIDS Res Hum Retrovir *10*: 1259-1268, 1994.
54 Brauweiler A, Garrus JE, Reed JC and Nyborg JK: Regression of bax gene expression by the HTLV-1 tax protein: implications for the suppression of apoptosis in viral infected cells. Virology *28*: 135-140, 1997.
55 de la Fuente C, Santiago F, Chong SY, Deng L, Mayhood T, Fu P, Stein D, Denny T, Coffman F, Azimi N, Mathieux R and Kashanchi F: Overexpression of p21 (waf-1) in human T-cell lymphotropic virus type 1 infected cells and its association with cyclin A/cdk2. J Virol *74*: 7270-7283, 2000.

Received March 31, 2003
Accepted October 13, 2003